

Electron-Spin Polarizations Generated from Interactions between Excited Triplet Porphyrins and Stable Radicals Studied by Time-Resolved Electron Paramagnetic Resonance

Jun-ichi Fujisawa, Yasunori Ohba, and Seigo Yamauchi*

Institute for Chemical Reaction Science, Tohoku University, Katahira 2-1-1, Aobaku, Sendai 980–77, Japan

Received: June 13, 1996; In Final Form: September 19, 1996[⊗]

Time-resolved EPR studies were made on CIDEP mechanisms in the system of excited triplets (T) and doublets (D) using various kinds of porphyrins and nitroxide radicals. The CIDEPs were investigated by observing both signals of T and D and discussed in terms of an electron-spin polarization transfer (ESPT) and a radical–triplet pair mechanism (RTPM). It is demonstrated for the first time that ESPT is actually existent by comparing the triplet and doublet CIDEP signals. The ESPT process was found to be diffusion-controlled in toluene and 2-butanol, and an effective distance for ESPT was estimated as $<11 \text{ \AA}$. For RTPM, an enhancement of CIDEP polarization was observed by axial ligation of radicals to zinc porphyrins. We also found novel CIDEP involving molecular oxygen, which is interpreted by RTPM between singlet molecular oxygen and stable radicals.

Introduction

Chemically induced dynamic electron polarization (CIDEP) is generated due to interactions between transient radicals that are produced in an early stage of a photochemical reaction. Analyses of CIDEP provide valuable information such as the structures, kinetics, and spin relaxations about reaction precursory excited states (S_1 or T_1), intermediate radical pairs, and radicals. Considerable effort has been devoted to study CIDEP mechanisms on various kinds of photoreactions by means of time-resolved EPR (TREPR).^{1,2} CIDEPs generated from a pair of radicals are interpreted by two major mechanisms of a triplet mechanism (TM)³ and a radical pair mechanism (RPM).⁴ In the former, an electron-spin polarization (ESP) generated in an excited triplet state due to anisotropic intersystem crossing (isc) between S_1 and T_1 is conserved on the produced radicals. In the latter, two kinds of ESPs, $S-T_0$ and $S-T_-$ types, are produced during encounters of radicals via singlet and triplet pair interactions. These CIDEP mechanisms are now almost established both from theories and experiments.^{1–4}

Recently, CIDEPs generated between an excited triplet (T) and a doublet (D) were reported in the literature.^{5–7} Two kinds of CIDEP mechanisms have been proposed: a radical triplet pair mechanism (RTPM)⁵ and an electron-spin polarization transfer (ESPT)^{6,7} In the RTPM, the polarization arises from interactions between quartet and doublet pairs that are generated by exchange couplings between T–D. The RTPM is analogous to the RPM in the sense that the ESP is generated by encounters of two paramagnetic species and has two kinds of mechanisms corresponding to $S-T_0$ and $S-T_-$ types in the D–D system. There are also two types of polarizations depending on the concerned excited states, such as $A + A/E$ and $E + E/A$ ($J < 0$) for S_1 and T_1 , respectively. Many studies on the RTPM have been made theoretically and experimentally.⁵

For the ESPT, the T_1 polarization generated by spin-selective isc is considered to be transferred to a radical via an exchange interaction between T–D, which resembles the TM in the D–D system. However, no experimental evidence had been reported yet for this mechanism. In a previous communication,⁷ we reported the first direct demonstration of ESPT in triplet

porphyrins and TEMPO systems. In this report, we represent full investigations on CIDEP mechanisms of both ESPT and RTPM involved in the T–D systems of various kinds of porphyrins and nitroxide radicals by means of TREPR.

We selected tetraphenylporphyrins (MTPP; $M = H_2, Mg, Zn, Cd$) and octaethylporphyrins (MOEP; $M = H_2, Zn$) as shown in Figure 1, because these porphyrins involve different T_1 polarizations depending on the central atoms. The T_1 polarizations of the porphyrins are reported to be absorptive for ZnTPP,^{8–12} CdTPP,¹¹ and ZnOEP¹¹ and emissive for H₂TPP,^{8,9} MgTPP,^{9–12} and H₂OEP.^{10,11} The emissive polarization means that a T_+ ($\alpha\alpha$) level in the triplet manifolds has more populations than those of a T_- ($\alpha\alpha$) level. For stable radicals, we used TEMPO (2,2,6,6-tetramethylpiperidine-1-oxyl, free radical), nitph (phenyl nitronyl nitroxide), and imph (phenyl imino nitroxide), which are also shown in Figure 1.

In this study, we aim at (1) investigating ESPT and RTPM by directly observing the CIDEP signals of T_1 porphyrins in solution together with those of the radicals, (2) analyzing a spin-exchange process between T and D by determining the rates of the ESPT in solvents of different viscosity, (3) examining the radical dependence of CIDEP effects, and (4) interpreting novel CIDEP involving molecular oxygen.

Experimental Section

H₂TPP, MgTPP, ZnTPP, CdTPP, ZnOEP, nitph, and imph were synthesized according to the methods described in the literature.^{13–15} TEMPO (Tokyo Kasei) and H₂OEP (Aldrich) were used as received. Spectral-grade toluene ($\eta^{298K} = 0.6 \text{ cP}$),^{16a} 2-butanol (4.2 cP),^{16a} 1-octanol (9 cP),^{16a} cyclohexanol (68 cP),^{16c} and liquid paraffin (170 cP)^{16b,c} were purchased from Wako Pure Chemicals and used as solvents without further purification. The concentrations of the porphyrins and radicals were 1×10^{-3} and $(0.1–10 \times 10^{-3} \text{ M})$, respectively. The solutions were deaerated by repeated freeze–pump–thaw cycles on the vacuum line.

TREPR and steady-state EPR measurements were carried out at room temperature using a modified X-band JEOL JES-FE2XG EPR spectrometer. The TREPR spectra and time-profiles of the signals were obtained by a NF BX-531 boxcar integrator and an Iwatsu DM-7200 digital memory, respectively. The details of the TREPR apparatus have been described

* To whom correspondence should be addressed.

[⊗] Abstract published in *Advance ACS Abstracts*, December 15, 1996.

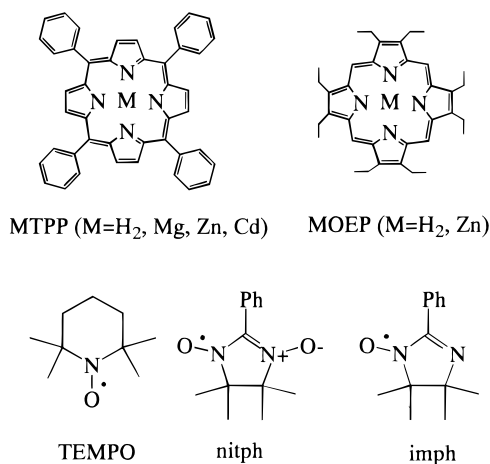


Figure 1. Structures of the porphyrins and stable radicals.

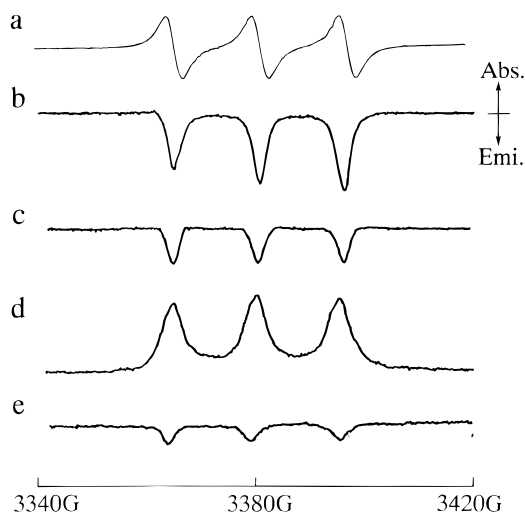


Figure 2. (a) Steady-state EPR spectrum of TEMPO and time-resolved EPR spectra observed in toluene for the H₂OEP (b, c) and ZnOEP-TEMPO (d, e) systems at 0.1–0.3 μ s (b, d) and 2.0–2.2 μ s (c, e).

previously.¹² A Lambda Physik LPD3000 dye laser ($\lambda = 580$ – 590 nm) pumped by a Lambda Physik LPX100i excimer laser was employed to excite the S₁ states of the porphyrins.

Results and Interpretation

1. Spectra and Decays. The steady-state and time-resolved (TR) EPR spectra observed at 0.1–0.3 and 2.0–2.2 μ s in the H₂OEP and ZnOEP systems are shown in Figure 2. The peak positions of the time-dependent signals were in good agreement with the steady-state signals of TEMPO ($g = 2.006$, $A_N = 15.5$ G). This result indicates clearly that the observed CIDEP spectra are due to the polarized TEMPO radical. The TREPR spectra show that the CIDEPs consist of two polarizations. The first polarizations with faster decays are an emission and an absorption of microwave for the H₂OEP and ZnOEP systems, respectively. The second polarizations with slower decays are emissions for both systems. The CIDEP signals of TEMPO were also observed for other porphyrin systems. Time-profiles of the CIDEP signals are shown in Figure 3. From the figure, it is found that the first polarizations are emissive for the H₂-TPP, MgTPP, and H₂OEP systems and absorptive for the ZnTPP, CdTPP, and ZnOEP systems and the second polarizations are emissive in all the systems. The decay times are found to be $0.4 \pm 0.1 \mu$ s for the first polarizations in all systems.¹⁷ In contrast, the second polarizations decay with a range of several microseconds to a few tens of microseconds depending on the system.

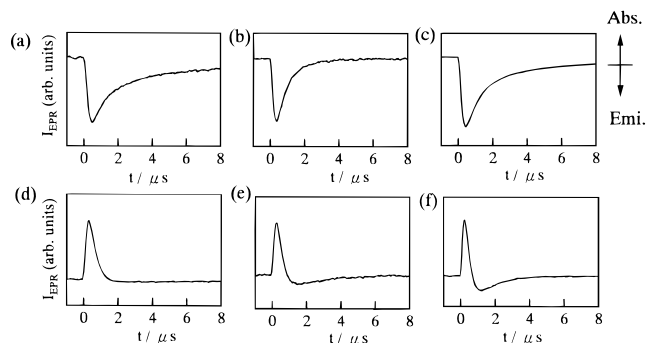


Figure 3. Time profiles of the TEMPO signals obtained for the (a) TEMPO–H₂TPP, (b) –MgTPP, (c) –H₂OEP, (d) –ZnTPP, (e) –CdTPP, and (f) –ZnOEP systems in toluene.

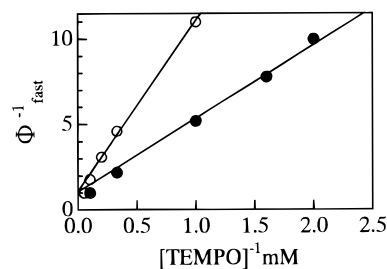


Figure 4. Plots of Φ_{fast}^{-1} vs $[\text{TEMPO}]^{-1}$ for the ZnTPP–TEMPO system in toluene (●) and 2-BuOH (○). See the text for the simulated lines.

2. Dependence on TEMPO Concentration. We examined the dependence of the magnitude of the first polarization on the TEMPO concentration in the ZnTPP–TEMPO system. The magnitude of the first polarization (I_{fast}) was measured, and the quantum yield (Φ_{fast}) was calculated as the ratio of the magnitude with respect to maximum (saturated) I_{fast} that is obtained under $[\text{TEMPO}] > 10$ mM; namely, $\Phi_{\text{fast}} \equiv I_{\text{fast}}(x \text{ mM})/I_{\text{fast}}(>10 \text{ mM})$. Plots of Φ_{fast}^{-1} vs $[\text{TEMPO}]^{-1}$ are presented in Figure 4 for toluene and 2-butanol solvents. Each plot was fitted by a linear function of Φ_{fast}^{-1} and $[\text{TEMPO}]^{-1}$ with an intercept of 1, as shown in the figure. The slopes of the straight lines are obtained as 4.4 and 10 mM for the toluene and 2-butanol systems, respectively.

For the second polarization, we observed hyperfine-dependent polarization E/A (an absorption and an emission of microwave at lower and higher fields, respectively) with a net emission (E) at lower concentrations (~ 0.5 mM) of TEMPO. However, the E/A polarization decreases with increasing the concentration of TEMPO and diminishes at higher concentrations (> 2 mM).

In the TREPR spectrum of the H₂OEP system the hyperfine-dependent polarization was observed at an earlier stage (0.1–0.3 μ s) after the laser excitation, as shown in Figure 2b. The TREPR spectra and time profiles of the TEMPO signals were observed at different TEMPO concentrations as shown in Figure 5. From the spectra, it is found that the emissive polarization decreases with increasing TEMPO and is absorptive at higher concentrations, where the peak ($m_l = -1$) at the higher field is more emissive than that ($m_l = +1$) at the lower field. The decay analysis with a double exponential function shows that the absorptive polarization decays with a time constant of $0.19 \pm 0.05 \mu$ s. These spectra are interpreted by a superposition of multiplet A/E and net A polarizations. The A/E polarization was diminished by an addition of 7% methyl iodide. The similar A/E polarization was also observed in the H₂TPP system.

3. Triplet Signals. We observed TREPR spectra of T₁ porphyrins for the first time in various kinds of liquid solutions. The spectra of ZnTPP observed at room temperature and 0.1–0.3 μ s are shown in Figure 6. In liquid paraffin, a TREPR

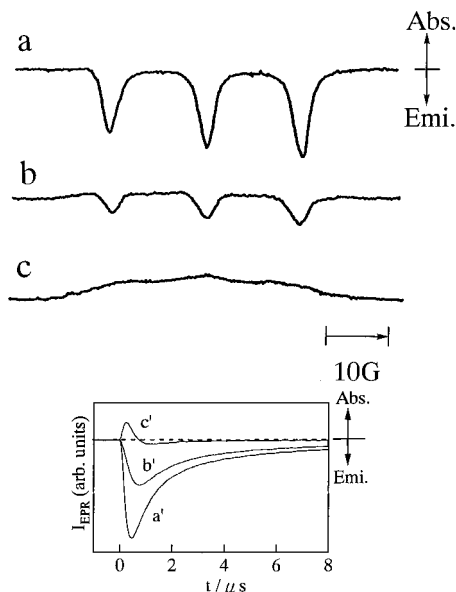


Figure 5. Time-resolved EPR spectra observed at 0.1–0.3 μs and time profiles of the higher field peak for the H_2OEP system in toluene with the TEMPO concentrations of 5 mM (a, a'), 10 mM (b, b'), and 20 mM (c, c').

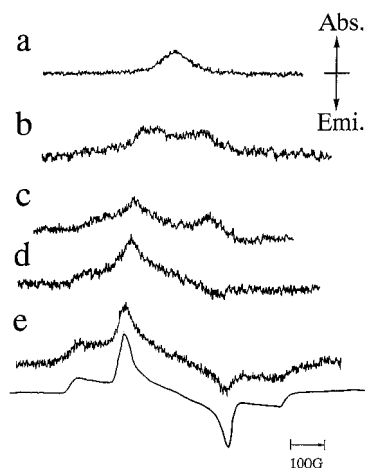


Figure 6. TREPR spectra of T_1 ZnTPP observed at 0.1–0.3 μs in (a) toluene, (b) 2-butanol, (c) 1-octanol, (d) cyclohexanol, and (e) liquid paraffin solutions and the simulated spectrum with $D = 0.93$ GHz, $E = 0$ GHz, and an isc ratio of $P_x:P_y:P_z = 0:0:1$.

spectrum was analyzed by a polarized T_1 ZnTPP with EPR parameters of $D = 0.93$ GHz and $E = 0$ GHz and an isc ratio of $P_x:P_y:P_z = 0:0:1$.¹⁸ Here x , y , and z are principal axes of the zero-field splitting, and z is perpendicular to the xy porphyrin plane. The TREPR spectra and decays of the signals are dependent on the viscosity of the solution.¹⁹ In toluene, a relatively broad peak ($\Delta H_{1/2} = \text{ca. } 90$ G) is observed and decays in ca. 50 μs , being independent of the microwave power. This signal is quenched efficiently by molecular oxygen, giving a decay time of 0.4 ± 0.1 μs under an atmosphere. The spectrum is assigned as that of T_1 ZnTPP, having a Boltzmann population (thermalized T_1). In the ZnTPP–TEMPO/toluene system, the thermalized T_1 ZnTPP signal was observed together with the polarized TEMPO signal and decayed with a time constant of 15 ± 2 μs at $[\text{TEMPO}] = 5$ mM, where the emissive second polarization on TEMPO decays with almost the same time constant (17 ± 2 μs).

In liquid paraffin, the polarized TEMPO signal was observed together with the signal of polarized T_1 porphyrin, as shown in Figure 7, where the time profiles of the TEMPO and T_1 ZnTPP signals are also shown. From the figures, it is easily found that the TEMPO polarization increases and the T_1 polarization

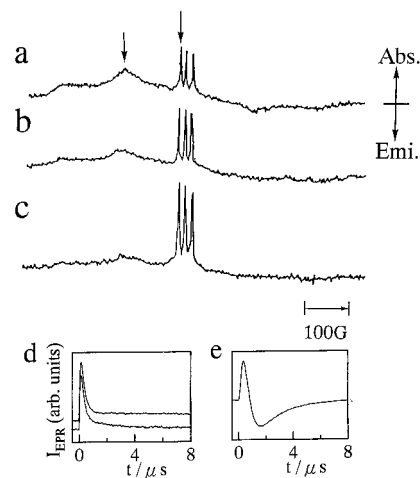


Figure 7. TREPR spectra observed at 0.1–0.3 μs for the ZnTPP systems in liquid paraffin with TEMPO of (a) 5, (b) 10, and (c) 20 mM. Time profiles of the CIDEP signals of the T_1 ZnTPP with no TEMPO (upper) and 5 mM TEMPO (lower) and the TEMPO signal are also shown in d and e, respectively, which are observed at the fields indicated by the arrows in the spectra.

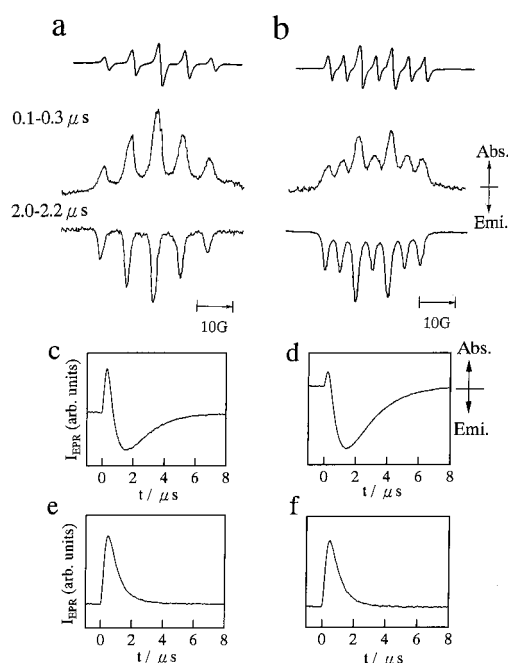


Figure 8. Steady-state EPR spectra (top) and TREPR spectra for the ZnTPP–nitph (a) and –imph (b) systems. Time profiles (lower) of the nitph (c) and imph (d) signals are also shown in toluene and in 0.1 M pyridine added toluene, e and f, respectively.

of ZnTPP decreases with increasing the TEMPO concentration. The time profile of the T_1 ZnTPP signal shows two components: one is an anomalous polarization due to non-Boltzmann distribution with a shorter decay time, and the other is due to thermalized T_1 ZnTPP with a longer decay time. The decay curves of the T_1 ZnTPP signals in $[\text{TEMPO}] = 0$ mM and 5 mM systems were analyzed by a double-exponential function as 0.28 ± 0.05 and 350 ± 2 μs and 0.23 ± 0.05 and 2.0 ± 0.2 μs , respectively. These results evidently indicate that both T_1 ZnTPPs with nonthermal and thermal distributions are quenched by TEMPO. The time profile of the TEMPO polarization was found to be analyzed by a triple-exponential function involving a rising part (0.28 ± 0.05 μs) and decaying parts (0.35 ± 0.05 and 1.7 ± 0.2 μs).

4. Radical Dependence. Figure 8 shows the steady-state EPR spectra and TREPR spectra at different delay times in ZnTPP and nitroxide radical systems. For nitph, the steady-

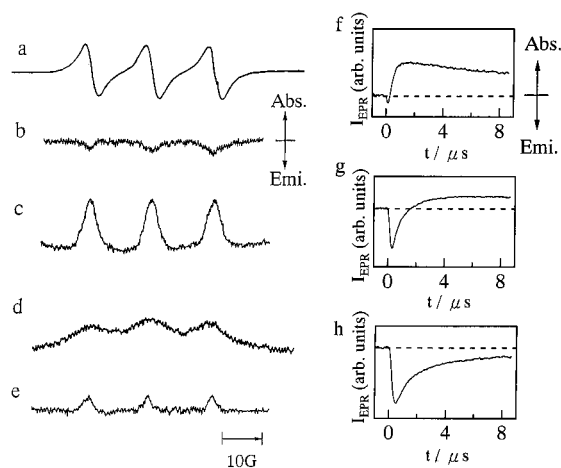


Figure 9. (a) Steady-state EPR spectrum of TEMPO and TREPR spectra observed at 0.1–0.3 (b, d) and 1.5–1.7 μs (c, e) for the H_2TPP and ZnTPP –TEMPO/air-saturated toluene systems, respectively. Time profiles of the TEMPO signals obtained under conditions of (f) air-saturated, (g) incomplete Ar bubbling, and (h) thoroughly deaerated toluene solutions are also shown for the H_2TPP –TEMPO system.

state EPR spectrum exhibits five lines ($g = 2.006$, $A_N = 7.4$ G) due to two equivalent nitrogen atoms. Seven lines ($g = 2.006$, $A_N = 9.2$ and 4.5 G) due to two nonequivalent nitrogen atoms were observed for *imph*. Similar to the ZnTPP –TEMPO system, two kinds of polarizations, net absorptions (A) and hyperfine dependent polarizations (E + E/A), were observed. The time profiles of the signals are also shown in Figure 8 and analyzed with double-exponential functions; the first polarizations are absorptive with decay times of 0.65 ± 0.1 and 0.60 ± 0.1 μs and the second ones emissive with decay times of 1.6 ± 0.1 and 1.9 ± 0.1 μs for the *nitph* and *imph* systems, respectively. It was found for the second polarizations of these systems that the decay times are shorter and the magnitudes are much larger than those of the TEMPO system. In order to examine the effect of axial ligation of the radicals to ZnTPP , the more acidic ligand pyridine (0.1 M) was added to the systems.^{21,22} The results were shown in parts e and f of Figure 8, where the second polarizations are found to disappear. These results show clearly that the second polarization is enhanced via an axial ligation of the radical, although the ligation is weak and no appreciable effects of the radicals are observed on the UV spectra. For the H_2TPP –*nitph* and –*imph* systems, no effects of pyridine were observed, indicating an involvement of some ligation in the ZnTPP system.

5. CIDEP Due to Oxygen. We found a noble polarization under an aerated condition. The TREPR spectra for the H_2TPP and ZnTPP –TEMPO/air-saturated toluene systems are shown in Figure 9. The observed CIDEPs are composed of two components. The first polarizations with faster decays were emissive and absorptive for the H_2TPP and ZnTPP systems, respectively, which agrees with those obtained for the deaerated systems. On the other hand, the second polarizations with slower decays showed absorptions of microwave for both of the systems, in contrast to emissions in the deaerated systems. Figure 9 shows the time profiles of the TEMPO signals observed under different concentrations of molecular oxygen: (a) air-saturated, (b) incomplete Ar bubbling, (c) completely deaerated in the H_2TPP –TEMPO system. A relative magnitude of the absorptive polarization decreases with decreasing the concentration of molecular oxygen and the signal diminishes in the deaerated sample. From the analyses of the decay curves, the decay times of the absorptive polarizations are obtained as 17 ± 3 and 21 ± 3 μs for the ZnTPP and H_2TPP /air-saturated toluene systems, respectively. We determined the decay times of singlet molecular oxygen by means of time-resolved thermal

lens spectroscopy²³ as 18 ± 3 and 20 ± 3 μs for the ZnTPP and H_2TPP –TEMPO/air-saturated toluene systems, respectively.

Discussion

1. Existence of ESPT. Two kinds of CIDEPs were observed at different decay times. The first polarizations with faster decays are in good agreement with the T_1 polarizations of the corresponding porphyrins. In all systems involving TEMPO, the decay times were 0.4 ± 0.1 μs , which is the same as the reported spin–lattice relaxation (SLR) time²⁴ (0.4 μs) of TEMPO within experimental error. The SLR time (~ 20 ns) of T_1 ZnTPP in less viscous solution²⁵ is known to be much shorter than that (0.4 μs) of TEMPO. Therefore, if the ESPT occurs from porphyrins to TEMPO, the TEMPO signal should decay with the SLR time of TEMPO.

In liquid paraffin, the polarized T_1 ZnTPP signal was observed together with the polarized TEMPO signal. The magnitude of the TEMPO polarization increases with quenching of polarized T_1 ZnTPP , which indicates clearly that the TEMPO polarization is related profoundly to the T_1 ZnTPP polarization. The reaction and spin dynamics of this system are considered to be expressed by the following scheme:



k_{ESPT} , k_{RTPM} , $k_{T_1}^{-1}$, k_{TEMPO}^{-1} , and k_d are taken as the rates of formation of TEMPO polarizations due to ESPT and RTPM, the SLR times of T_1 ZnTPP and TEMPO, and the decay rate constant of T_1 ZnTPP , respectively. # stands for a polarized species. Here we regarded reactions 1 and 4 as the pseudo-first-order reactions because $[\text{TEMPO}] \gg [{}^3\text{P}]$. From the scheme, the time evolution of the TEMPO polarization is described by the following differential equation:

$$\frac{d[\text{TEMPO}^\#]}{dt} + k_{\text{TEMPO}}[\text{TEMPO}^\#] = A_1 \exp\{-(k_{T_1} + k_{\text{ESPT}})t\} + A_2 \exp(-k_d t) \quad (6)$$

An analytical solution to eq 6 is expressed by a triple-exponential function as²⁶

$$[\text{TEMPO}^\#] = A_3 \exp\{-(k_{T_1} + k_{\text{ESPT}})t\} + A_4 \exp(-k_{\text{TEMPO}}t) + A_5 \exp(-k_d t) \quad (7)$$

Here, A_1 , A_2 , A_3 , A_4 , and A_5 are constants. As described in the previous section, the decay curve was fitted by the triple exponential function with the parameters 0.28 ± 0.05 , 0.35 ± 0.05 , and 1.7 ± 0.2 μs . The values of 0.28 and 1.7 μs coincide with those of $(k_{T_1} + k_{\text{ESPT}})^{-1}$ (0.23 μs) and k_d^{-1} (2.0 μs) within experimental errors, respectively, that were obtained from a decay of the T_1 ZnTPP signal in liquid paraffin.

The results for the first polarizations of TEMPO are summarized as follows. (1) The polarities are in agreement with those of the T_1 polarizations of the corresponding porphyrins. (2) The decay times are the same as the spin–lattice relaxation time of TEMPO. (3) The intensity increases with quenching of the T_1 polarization. (4) The rise time (0.28 μs) coincides with the decay time (0.23 μs) of the polarized T_1 ZnTPP signal

in liquid paraffin solution. These results lead us distinctly to the conclusion that the first polarization is due to ESPT from T_1 porphyrins to TEMPO.

2. Rate of ESPT. From the relation between the magnitude of the ESPT polarization and the TEMPO concentration, we estimate the rate of ESPT. The inverse of the yield of ESPT, Φ_{ESPT}^{-1} , is expressed as

$$\Phi_{\text{ESPT}}^{-1} = 1 + k_{T_1}/(k_{\text{ESPT}}[\text{TEMPO}]) \quad (8)$$

where k_{T_1}/k_{ESPT} was determined to be 4.4 and 10 mM in toluene and 2-butanol solutions, respectively, from Figure 4. The $k_{T_1}^{-1}$ of T_1 ZnTPP is calculated to be 21 and 80 ns in toluene and 2-butanol, respectively, from the equation^{3b} of Atkins and Evans using $k_{T_1}^{-1}$ (28 ns)²⁵ in ethanol. Then, the rates of ESPT (k_{ESPT}^{-1}) are determined to be 1.1×10^{10} and $1.3 \times 10^9 \text{ M}^{-1} \text{ s}^{-1}$ in toluene and 2-butanol, respectively. The diffusion rates,²⁷ k_{diff} , are calculated to be 1.3×10^{10} (toluene) and $1.9 \times 10^9 \text{ M}^{-1} \text{ s}^{-1}$ (2-butanol) from the reported viscosities (0.6 and 4.2 cP, respectively) at room temperature. The rates of ESPT are in good agreement with the corresponding diffusion rates.

The result that the ESPT occurs via spin exchange between T and D with the diffusion rate indicates that the spin exchange occurs promptly on an each encounter between T and D and $2J \gg k_{\text{diff}}$. Here $2J$ denotes an exchange parameter for Q_1 and D_1 .^{5f} J is generally expressed as

$$J = J_0 \exp\{-\lambda(r - d)\} \quad (9)$$

J_0 is the J value at the closest approach ($r = d$). When $2J = k_{\text{diff}}$ ($6.5 \times 10^7 \text{ s}^{-1}$) at $[\text{TEMPO}] = 5 \text{ mM}$ in toluene, we calculate the distance (r) as 11 Å using the parameters^{5f} of $\lambda = 0.8 \text{ Å}^{-1}$, $J_0 = 8.0 \times 10^8 \text{ s}^{-1}$, and $d = 7 \text{ Å}$ for the T–D system reported by Goudsmit et al. For the present case of $2J \gg k_{\text{diff}}$, the effective distance is estimated to be $<11 \text{ Å}$, which is close to the sum of the van der Waals radii (7 Å)²⁷ of ZnTPP and TEMPO, indicating that close contact is important for the ESPT.

3. RTPM. The second polarizations with slower decays are net emissions for all systems and exhibit hyperfine-dependent multiplet polarizations (E/A) at lower concentrations of TEMPO. For the ZnTPP–TEMPO system, the decay time ($17 \pm 2 \mu\text{s}$) of the second polarization agrees with that ($15 \pm 2 \mu\text{s}$) of T_1 ZnTPP. In highly viscous liquid paraffin ($\eta^{293\text{K}} = 170 \text{ cP}$) and less viscous toluene ($\eta^{293\text{K}} = 0.6 \text{ cP}$) solutions, it is found that both T_1 polarizations and T_1 populations are quenched effectively with TEMPO. Interestingly, the quenching of T_1 ZnTPP was more effective in liquid paraffin (2.0 μs) than that (17 μs) in toluene, indicating that the triplet quenching is remarkably dependent on the viscosity of the solution. For the second polarization, the results are summarized as (1) the polarizations are E + E/A for all the systems and (2) the decay rate constants are the same as those of the thermalized T_1 ZnTPP signals in both toluene and liquid paraffin. From these results, it is clearly indicated that the second polarization is due to RTPM with the triplet precursor under $J < 0$. The multiplet polarization decreases in proportion to the concentration of TEMPO, which is explained by an average of populations occurring among the hyperfine levels of TEMPO via electron-spin exchange interactions.³¹ This result indicates that the spin-exchange interaction has to be considered for quantitative analyses of the multiplet polarization due to the RTPM.^{5f}

The hyperfine-dependent A/E polarization is observed at earlier times and diminished by an addition of methyl iodide (MeI) in the H_2OEP , and H_2TPP –TEMPO systems. The net absorptive polarization appears obviously at the higher TEMPO concentration (20 mM) and decays with almost the same time

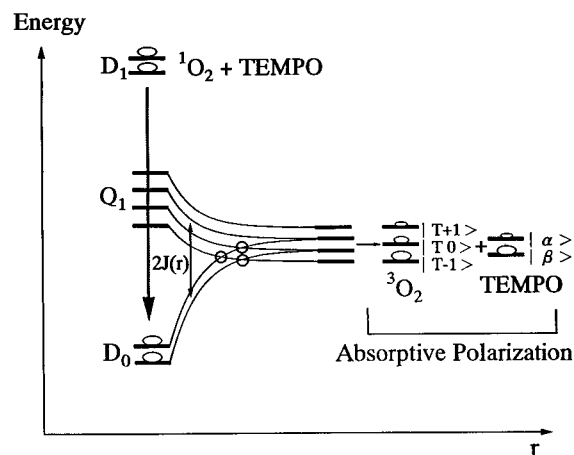


Figure 10. Energy diagram and a mixing scheme of molecular oxygen and a radical for the RTPM with $J < 0$.

constant (0.19 μs) as the reported SLR time (ca. 0.11 μs)^{24c} of TEMPO at 20 mM. These A + A/E polarizations are interpreted by the RTPM with a singlet precursor under $J < 0$ as the following.

The S_1 lifetimes of H_2OEP , H_2TPP , MgTPP , ZnTPP , ZnOEP , and CdTPP are reported to be 22, 14, 9.2, 2.7, 2.5, and 0.065 ns,³² showing that the S_1 lifetimes of H_2TPP and H_2OEP are longer than those of other porphyrins. It is also reported that S_1 ZnOEP is quenched by 20% MeI with a decay time of 0.87 ns.^{32d} Since the S_1 lifetime is much shorter than the SLR time of TEMPO, the polarization due to the RTPM with the singlet precursor should decay with the SLR time of TEMPO. The diffusion rate of $6.5 \times 10^7 \text{ s}^{-1}$ obtained at $[\text{TEMPO}] = 5 \text{ mM}$ in toluene is comparable to the decay rates of S_1 H_2OEP and H_2TPP . All these considerations support the concern of the RTPM with the singlet precursor.

4. Radical Dependence. The CIDEPs due to the ESPT and the RTPM with the triplet precursor were also observed for the ZnTPP–nitph and –imph systems. The decay times of the polarizations due to the ESPT were found to be 0.65 ± 0.1 and $0.60 \pm 0.1 \mu\text{s}$, which are assigned to the SLR times of nitph and imph, respectively, being similar to the TEMPO system. These are the first reported SLR times for these radicals. Thus, a measurement of the decay of the ESPT signal provides such valuable information on spin dynamics of involved radicals. The second RTPM polarizations suffer more striking effects of pyridine in the ZnTPP system than those of the TEMPO case. This is interpreted by the fact that the nitph and imph radicals approach much closer to the porphyrins than the TEMPO radical via an axial ligation on the encounters.

5. Oxygen Effect. Unusual CIDEP was observed on TEMPO for the porphyrin–TEMPO systems under molecular oxygen. The results for this polarization are summarized as follows. (1) The polarity is absorptive and independent of the kind of porphyrins. (2) The decay times are analyzed to be 17 ± 3 and $21 \pm 3 \mu\text{s}$ for the ZnTPP and H_2TPP /air-saturated toluene systems, respectively. (3) The lifetime of T_1 ZnTPP is $0.4 \pm 0.1 \mu\text{s}$ in the ZnTPP/air-saturated toluene system. (4) Singlet molecular oxygen was found to be quenched by TEMPO such that the lifetime decreases from 29 μs ³³ to 18 μs under $[\text{TEMPO}] = 5 \text{ mM}$ in the ZnTPP system and the decay times in the ZnTPP and H_2TPP –TEMPO/air-saturated toluene systems are in agreement with the decays of the TEMPO polarizations. (5) The polarity is the same as that of the CIDEP due to the RTPM with the singlet precursor under $J < 0$.

A proposed interaction scheme between singlet molecular oxygen and TEMPO is shown in Figure 10. Singlet molecular

oxygen is quenched by TEMPO, providing more populations in the D_0 state. Mixings of the Q_1 and D_0 states with molecular oxygen via spin–spin interactions give rise to net absorptive polarization. From these results, it is demonstrated evidently that the new polarization is generated by the RTPM between TEMPO and singlet molecular oxygen.

Lastly, we consider the reason why the ESPT polarization is easily observed in the porphyrin and radical systems. The magnitude of the ESPT is dependent on both the T_1 polarization and the SLR of the T_1 state. Porphyrins have slower rotational correlation times due to their large sizes ($r \sim 5 \text{ \AA}$),²⁹ which is considered to provide a moderate T_1 polarization and a slower spin–lattice relaxation time even in solution. These expectations are clearly demonstrated by the TREPR spectra of the T_1 state (Figure 6) observed in various solutions. Further, in the porphyrin systems, the T_1 energies are located within the range of $11\,000\text{--}14\,000 \text{ cm}^{-1}$ ^{32a,b,34} and are lower than those of the D_1 states of the radicals, $18\,000 \text{ cm}^{-1}$ ³⁵ for TEMPO, ca. $14\,000 \text{ cm}^{-1}$ ³⁶ for nitph, and ca. $18\,000 \text{ cm}^{-1}$ ³⁶ for imph. If T_1 is higher than D_1 in energy, an energy transfer³⁵ is known to occur promptly from T_1 to D_1 , giving very large RTPM polarizations. This leads us into difficulty in an unambiguous assignment of ESPT. These combined effects in dynamics and energetics are considered to make ESPT observations easier in our system.

Conclusion

An electron-spin polarization transfer (ESPT) was investigated thoroughly by using various kinds of porphyrins and radicals. Direct observations of the EPR signals of T_1 porphyrins in solution enable us to analyze unambiguously the CIDEP appeared on the radicals. On the basis of much definitive evidence, we proved the existence of ESPT in our system. The rate of the ESPT due to spin exchange interactions was determined to be diffusion-controlled, and a close contact of the T_1 porphyrin and the radical was indicated for this process.

The RTPM polarization was also analyzed in these systems. Both polarizations with triplet and singlet precursors were observed depending on the system. From the effect of pyridine, it is indicated that axial ligation is important for the RTPM involving nitph and imph radicals. We found novel CIDEP induced by molecular oxygen, which is assigned as the RTPM generated from an interaction between singlet oxygen and the radical.

Acknowledgment. We thank Associate Professor Masahide Terazima at Kyoto University for his help in the thermal lens experiment. This work was supported by a Grant-in-Aid for Scientific Research on Priority Area "Photoreaction Dynamics" (No. 08218206) from the Ministry of Education, Science and Culture, Japan.

References and Notes

- (1) Muus, L. T.; Atkins, P. W.; McLauchlan, K. A.; Pedersen, J. B. *Chemically Induced Magnetic Polarization*; Reidel: Dordrecht, The Netherlands, 1977.
- (2) Salikhov, K. M.; Molin, Y. N.; Sagdeev, R. Z.; Buchachenko, A. L. *Spin Polarization and Magnetic Effects in Radical Reactions*; Elsevier: Amsterdam, 1984.
- (3) (a) Wong, S. K.; Hutchison, D. A.; Wan, J. K. S. *J. Chem. Phys.* **1973**, *59*, 985. (b) Atkins, P. W.; Evans, G. T. *Mol. Phys.* **1974**, *27*, 1633.
- (4) (a) Adrian, F. J. *J. Chem. Phys.* **1971**, *54*, 3918. (b) Adrian, F. J.; Monchick, L. *J. Chem. Phys.* **1979**, *71*, 2600.
- (5) (a) Blättler, C.; Jent, F.; Paul, H. *Chem. Phys. Lett.* **1990**, *166*, 375. (b) Kawai, A.; Okutsu, T.; Obi, K. *J. Phys. Chem.* **1991**, *95*, 9130. (c) Kawai, A.; Obi, K. *J. Phys. Chem.* **1992**, *96*, 52; *Res. Chem. Intermed.*

- 1993**, *19*, 865. (d) Turro, N. J.; Khudyakov, I. V.; Bossmann, S. H.; Dwyer, D. W. *J. Phys. Chem.* **1993**, *97*, 1138. (e) Shushin, A. I. *Z. Phys. Chem.* **1993**, *182*, 9. (f) Goudsmid G.-H.; Paul, H.; Shushin, A. I. *J. Phys. Chem.* **1993**, *97*, 13243. (g) Rozenshtein, V.; Zilber, G.; Rabinovitz, M.; Levanon, H. *J. Am. Chem. Soc.* **1993**, *115*, 5193.
- (6) (a) Imamura, T.; Onitsuka, O.; Obi, K. *J. Phys. Chem.* **1986**, *90*, 6741. (b) Jenks, W. S.; Turro, N. *J. Res. Chem. Intermed.* **1990**, *13*, 237.
- (7) Fujisawa, J.; Ishii, K.; Ohba, Y.; Iwaizumi, M.; Yamauchi, S. *J. Phys. Chem.* **1995**, *99*, 17082.
- (8) Levanon, H. *Rev. Chem. Intermed.* **1987**, *8*, 287.
- (9) Levanon, H.; Norris, J. R. *Chem. Rev.* **1978**, *78*, 185.
- (10) Levanon, H.; Regev, A.; Galilii, T.; Hugerat, M.; Chang, C. K.; Fajer, J. *J. Phys. Chem.* **1993**, *97*, 13198.
- (11) Yamauchi, S.; Fujisawa, J. Unpublished results.
- (12) Yamauchi, S.; Ueda, T.; Satoh, M.; Akiyama, K.; Tero-kubota, S.; Ikegami, Y.; Iwaizumi, M. *J. Photochem. Photobiol. A: Chem.* **1992**, *65*, 177.
- (13) Adler, A. D.; Longo, F. R.; Finarelli, J. D.; Goldmacher, J.; Assour, J.; Korsakoff, L. *J. Org. Chem.* **1967**, *32*, 476.
- (14) Douough, G. D.; Miller, J. R.; Huennenkens, F. M. *J. Am. Chem. Soc.* **1951**, *73*, 4315.
- (15) (a) Ullman, E. F.; Call, L.; Osiecki, J. H. *J. Org. Chem.* **1970**, *35*, 3623. (b) Ullman, E. F.; Osiecki, J. H.; Boocock, D. G.; Darcy, R. *J. Am. Chem. Soc.* **1972**, *94*, 7049.
- (16) (a) Weissberger, A.; Proskauer, E. S.; Riddick, J. A.; Toops, E. E., Jr. *Technique of Organic Chemistry*, vol. VII. *Organic Solvents*, 2nd ed.; Interscience: New York, 1955. (b) Osborne, A. D.; Porter, G. *Proc. R. Soc. London, Ser. A* **1965**, *284*, 9. (c) Birks, J. B.; Salet, M. *J. Phys. B. Atom. Molec. Phys.* **1970**, *3*, 417.
- (17) The very weak emissive signal for the ZnTPP system is due to an overlap of an absorptive triplet signal as described in the Results and Interpretation section.
- (18) The E value of T_1 ZnTPP was obtained as 0.29 GHz at 77 K in toluene. Both effects of molecular rotations and electron hoppings between the Jahn–Teller split triplet states were observed from the temperature dependence of the spectrum, providing $E = 0$ GHz.
- (19) The change of the T_1 ZnTPP spectra must come from rotational motions in liquid solution.²⁰ The simulation of the spectra is now in progress.
- (20) Freed, J. F.; Bruno, G.; Polnaszek, C. *J. Chem. Phys.* **1971**, *55*, 5270.
- (21) The equilibrium constant for axial ligation of pyridine with ZnTPP is reported to be ca. 6000 M^{-1} at 298 K in ref 22, from which more than 99% ZnTPP ligates with pyridine.
- (22) Miller, J. R.; Dorough, G. D. *J. Am. Chem. Soc.* **1952**, *74*, 3977.
- (23) Terazima, M. *Chem. Phys. Lett.* **1994**, *230*, 87.
- (24) (a) Huisjen, M.; Hyde, J. S. *Rev. Sci. Instrum.* **1974**, *45*, 669. (b) Schwartz, R. N.; Jones, L. L.; Bowman, M. K. *J. Phys. Chem.* **1979**, *83*, 3429. (c) Koptuyg, I. V.; Bossman, S. H.; Turro, N. J. *J. Am. Chem. Soc.* **1996**, *118*, 1435.
- (25) van Willigen, H.; Levstein, P. R.; Ebersole, M. H. *Chem. Rev.* **1993**, *93*, 173.
- (26) Steinfeld, J. I.; Francisco, J. S.; Hase, W. L. *Chemical Kinetics and Dynamics*; Prentice-Hall: Englewood Cliffs, NJ, 1989; Chapter 2.
- (27) Diffusion rates are calculated by the Smoluchowski equation²⁸ as $k_{\text{diff}} = 4 \times 10^{-3} \pi (r_A + r_B)(D_A + D_B)N_A$ for the encounter process $A + B \rightarrow AB$. $r_A + r_B$ is an encounter cross section, D_A and D_B are the diffusion coefficients of A and B, respectively, and N_A is the Avogadro's number. The diffusion coefficient D is given by the Stokes–Einstein relation. In our systems, r_{ZnTPP} and r_{TEMPO} are taken to be 5 and 2 Å as reported in refs 29 and 30, respectively.
- (28) Smoluchowski, M. *Z. Phys. Chem.* **1917**, *92*, 129.
- (29) Dutt, G. B.; Periasamy, N. *J. Chem. Soc., Faraday Trans.* **1991**, *87*, 3815.
- (30) Hwang, J. S.; Mason, R. P.; Hwang, L.-P.; Freed, J. H. *J. Phys. Chem.* **1975**, *79*, 489.
- (31) Atherton, N. M. *Principles of Electron Spin Resonance*; Ellis Horwood: New York; Chapter 9.
- (32) (a) Harriman, A. *J. Chem. Soc., Faraday Trans. 2* **1980**, *76*, 1978. (b) Harriman, A. *J. Chem. Soc., Faraday Trans. 2* **1981**, *77*, 1281. (c) Gentemann, S.; Medforth, C. J.; Forsyth, T. P.; Nurco, D. J.; Smith, K. M.; Fajer, J.; Holten, D. *J. Am. Chem. Soc.* **1994**, *116*, 7363. (d) Rodrigueuz, J.; Kirmaier, C.; Holten, D. *J. Am. Chem. Soc.* **1989**, *111*, 6500.
- (33) Bishop, S. M.; Beeby, A.; Parker, A. W.; Foley, M. S.; Phillips, D. *J. Photochem. Photobiol. A: Chem.* **1995**, *90*, 39.
- (34) (a) Gouterman, M. In *The Porphyrins*; Dolphin, D., ed.; Academic: New York, 1978; Vol. 3, Chapter 1. (b) Ohno, O.; Kaizu, Y.; Kobayashi, H. *J. Chem. Phys.* **1985**, *82*, 1779. (c) Yamauchi, S.; Matsukawa, Y.; Ohba, Y.; Iwaizumi, M. *Inorg. Chem.* **1996**, *35*, 2910.
- (35) (a) Watkins, A. R. *Chem. Phys. Lett.* **1974**, *29*, 526. (b) Kuzmin, V. A.; Tatikolov, A. S. *Chem. Phys. Lett.* **1978**, *53*, 606.
- (36) These values were obtained from the UV spectra.